

Derivation of a non-local interfacial model for 3D wetting in an external field

N R Bernardino^{1,2}, A O Parry³, C Rascón⁴ and J M Romero-Enrique⁵

¹ Max-Planck-Institut für Metallforschung, Heisenbergstrasse 3, D-70569 Stuttgart, Germany

² Institut für Theoretische und Angewandte Physik, Universität Stuttgart, Pfaffenwalding 57, D-70569 Stuttgart, Germany

³ Department of Mathematics, Imperial College London, London SW7 2BZ, UK

⁴ Grupo Interdisciplinar de Sistemas Complejos (GISC), Departamento de Matemáticas, Universidad Carlos III de Madrid, E-28911 Leganés, Madrid, Spain

⁵ Departamento de Física Atómica, Molecular y Nuclear, Universidad de Sevilla, Apartado de Correos 1065, E-41080 Seville, Spain

Received 8 July 2009, in final form 29 September 2009

Published 26 October 2009

Online at stacks.iop.org/JPhysCM/21/465105

Abstract

We extend recent studies of 3D short-ranged wetting transitions by deriving an interfacial Hamiltonian in the presence of an arbitrary external field. The binding potential functional, describing the interaction of the interface and the substrate, can still be written in a diagrammatic form, but now includes new classes of diagrams due to the coupling to the external potential, which are determined exactly. Applications to systems with long-ranged (algebraically decaying) and short-ranged (exponentially decaying) external potentials are considered at length. We show how the familiar ‘sharp-kink’ approximation to the binding potential emerges, and determine the corrections to this arising from interactions between bulk-like fluctuations and the external field. A connection is made with earlier local effective interfacial Hamiltonian approaches. It is shown that, for the case of an exponentially decaying potential, non-local effects have a particularly strong influence on the approach to the critical regime at second-order wetting transitions, even when they appear to be sub-dominant. This is confirmed by Monte Carlo simulation studies of a discretized version of a non-local interfacial model.

(Some figures in this article are in colour only in the electronic version)

1. Introduction

A particularly subtle problem in interfacial phenomena is the description of the critical wetting transition with short-range forces in three dimensions [1–3]. Predictions of non-universal critical singularities based on renormalization group studies of local interfacial Hamiltonian models [4, 5] contrast sharply with the results of extensive Monte Carlo simulations of wetting in the 3D Ising model, which instead reveal only mild deviations from mean-field behaviour [6–8]. Recently, however, some progress has been made towards solving this discrepancy. In a series of recent papers [9–14], we have shown how a non-local interfacial Hamiltonian for 3D short-ranged wetting may be derived explicitly from an underlying Landau–Ginzburg–Wilson (LGW) model using Green’s function techniques. Within this description, the

binding potential, describing the interaction of the interface (upper wavy line) and a non-planar wall (lower wavy line), can be written as the diagrammatic expansion

$$W = a \text{ } \mathcal{Z} + b \text{ } \mathcal{V} + \dots, \quad (1)$$

which represents different classes of tube-like fluctuation that zig-zag between the interface and the wall. This approach highlights the importance of non-local effects at wetting transitions and, in particular, the role played by two-body-like interfacial interactions. These are characterized by a diverging length scale, missing in simpler local approaches, which has important damping influences on fluctuation effects.

In this paper, we generalize the derivation and analysis of the interfacial model to allow for the presence of an arbitrary external field $V(\mathbf{r})$. Our analysis is restricted to

short-ranged fluid–fluid (or Ising-like spin–spin) systems, but now considers different types of wall–fluid interaction. As we shall show, it is still possible to determine exactly the new form of the binding potential functional W and write this as a generalized diagrammatic expansion. Two applications of this formalism are considered in detail. Firstly, we consider the case of a long-ranged algebraically decaying external potential. Here, we are able to show how the familiar and oft-used ‘sharp-kink’ approximation emerges directly from the exact analysis and determine the corrections to it for arbitrary interfacial and wall configurations. For the particular case of a planar interfacial configuration near a planar wall, our result is in perfect agreement with earlier studies by Dietrich and Napiórkowski [15]. Next, we consider the very interesting case of an exponentially decaying wall potential, similar to earlier (local interfacial) studies by Aukrust and Hauge [16]. As with systems with short-ranged (contact) wall–fluid forces, this type of potential is also believed to exhibit (and actually enhance) non-universal critical effects at 3D wetting transitions. For example, even the underlying mean-field-like criticality shows strong non-universal behaviour. Our motivation here is to understand whether it is possible to ‘turn off’ non-local two-body interfacial interactions for specific ranges of the external field. If so, this would have potentially important implications for the observation of fluctuation-induced non-universality arising from interfacial fluctuations. However, even when two-body-like interfacial interactions are sub-dominant, we show that non-local effects are still highly important in the approach to the critical regime, and dampen strongly fluctuation effects.

2. Derivation of a non-local model with an external field

The starting point of the derivation of the non-local (NL) interfacial model is a continuum Landau–Ginzburg–Wilson Hamiltonian based on a magnetization-like order parameter $m(\mathbf{r})$:

$$H_{\text{LGW}}[m] = \int d\mathbf{r} \left\{ \frac{1}{2} (\nabla m)^2 + \Delta\phi(m) - \epsilon V(\mathbf{r})m \right\}. \quad (2)$$

The potential $\phi(m)$ models the bulk coexistence of fluid-like phases α and β with order parameters $-m_0$ and $+m_0$, respectively (which, for simplicity, we assume exhibit Ising symmetry). The shifted potential $\Delta\phi(m) = \phi(m) - \phi(m_0)$ conveniently subtracts the bulk contribution to the free energy (proportional to the volume). Following our earlier analysis [10] it is simplest to consider a double-parabola (DP) approximation for $\Delta\phi(m)$, which in zero-bulk field ($h = 0$) is

$$\Delta\phi(m) = \frac{\kappa^2}{2} (|m| - m_0)^2 \quad (3)$$

where κ is the inverse bulk correlation length. It is known that the DP approximation suffices to capture the critical singularities at wetting transitions. However, one may also use it as the starting point for a perturbative treatment of higher-order terms in $\Delta\phi(m)$ if so desired [11]. The main advantage of the DP approximation is that all the terms in

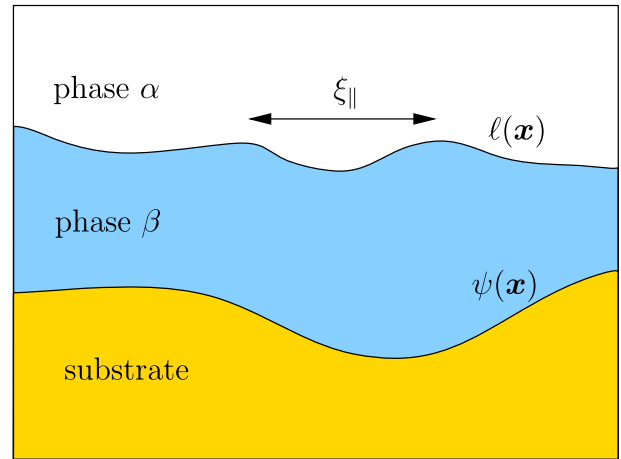


Figure 1. Schematic illustration of a wetting layer of phase β adsorbed on a substrate. The interfacial configuration is described by a function $\ell(x)$ and the substrate by $\psi(x)$. The length ξ_{\parallel} characterizes the height–height correlations of the interface.

the binding potential functional can be calculated and ordered systematically.

The LGW Hamiltonian now includes a coupling with an external field $V(\mathbf{r})$ with strength ϵ , which generalizes our previous analysis and will allow us to consider wetting with long-ranged wall–fluid interactions. In addition, we suppose the system is bounded by a wall described by a height function $\psi = \psi(x)$ which is often conveniently measured above some plane with parallel displacement $x = (x, y)$ (see figure 1). In most circumstances of course, the external potential depends on the wall shape itself so that more correctly we should write $V = V(\mathbf{r}; [\psi])$ to stress its functional dependence on the wall shape. This will be assumed implicitly. We also suppose that the magnetization on the boundary is *fixed*:

$$m(\mathbf{r}) = m_1, \quad \text{for } \mathbf{r} = (x, \psi(x)). \quad (4)$$

Without loss of generality, we assume that $m_1 > 0$ so the wetting layer forms at the wall– α interface for which the bulk magnetization is $-m_0$. This choice of fixed boundary condition is easiest to implement using the method discussed here and allows the non-local nature of the interfacial model to be derived most cleanly. In the absence of an external potential term, the condition $m_1 = m_0$ represents the mean-field critical wetting phase boundary for planar wall– α interfaces. Other choices of boundary condition can also be considered using Green’s function method [11].

Following Fisher and Jin [17, 18], we adopt a crossing criterion definition of the interface location which identifies it as the surface of zero iso-magnetization. Thus we consider constrained magnetization profiles for which

$$m(\mathbf{r}) = 0 \quad \text{for } \mathbf{r} = (x, \ell(x)), \quad (5)$$

where $\ell(x)$ is the interfacial height (see figure 1). The interfacial Hamiltonian is formally defined via a partial trace over Boltzmann weighted configurations which respect the

crossing criterion. A saddle point evaluation of the constrained sum leads to the Fisher–Jin identification:

$$H[\ell, \psi] = H_{\text{LGW}}[m_{\Xi}(\mathbf{r})] - F_{w\beta}[\psi] \quad (6)$$

where we have subtracted off a surface term corresponding to the excess free energy of the wall– β interface $F_{w\beta}[\psi]$, which is explicitly determined in our calculation. In the above identification, m_{Ξ} is the constrained profile that minimizes the LGW model subject to the crossing criterion and boundary condition. Within the DP approximation, this satisfies the Helmholtz equations

$$\begin{aligned} \nabla^2 m_{\Xi} &= \kappa^2(m_{\Xi} - m_0) - \epsilon V(\mathbf{r}), & m_{\Xi} > 0 \\ \nabla^2 m_{\Xi} &= \kappa^2(m_{\Xi} + m_0) - \epsilon V(\mathbf{r}), & m_{\Xi} < 0 \end{aligned} \quad (7)$$

with appropriate boundary conditions in the bulk and at the interface and wall.

These linear equations can be solved using Green’s function method similar to that described in [10, 11], but now with an additional particular solution term arising from the presence of the external field $V(\mathbf{r})$. These new contributions can also be expressed diagrammatically. For example, above the $\alpha\beta$ interface:

$$m(\mathbf{r}) + m_0 = m_0 \text{---} \text{---} + \frac{\epsilon}{2\kappa^2} \left(\text{---} \text{---} - \text{---} \text{---} \right), \quad (8)$$

which satisfies the boundary conditions to exponential accuracy in the radii of curvature [10]. The first diagram is the contribution for zero external field and has the algebraic expression:

$$\text{---} \text{---} = \int ds_{\ell} K(\mathbf{r}_{\ell}, \mathbf{r}) \quad (9)$$

where \mathbf{r}_{ℓ} denotes a point at the interface and $\int ds_{\ell}$ a surface integration with the appropriate area element $ds_{\ell} = dx\sqrt{1 + (\nabla\ell(x))^2}$. In the diagram, the upper and lower wavy lines represent the interface and substrate, respectively. The thick straight line represents Green’s function:

$$K(\mathbf{r}_1, \mathbf{r}_2) = \frac{\kappa}{2\pi|\mathbf{r}_1 - \mathbf{r}_2|} e^{-\kappa|\mathbf{r}_1 - \mathbf{r}_2|} \quad (10)$$

between points \mathbf{r}_{ℓ} (black circle) and \mathbf{r} (white circle). A filled black circle located on a surface represents an integral over that surface with the appropriate area element.

The final two diagrams have a similar algebraic interpretation, which now involves the external potential, which we write diagrammatically

$$V(\mathbf{r}) \equiv \text{---} \text{---} \quad (11)$$

where the wavy line represents the substrate. This notation is used to emphasize that in many applications the external field position \mathbf{r} arises from an integral of two-body forces between the point \mathbf{r} and every point in the solid substrate. Thus, for example, the last diagram in (8) represents the expression

$$\text{---} \text{---} - \text{---} \text{---} = \int ds_{\ell} K(\mathbf{r}, \mathbf{r}_{\ell}) \int_{V^+} d\mathbf{r}' \kappa K(\mathbf{r}', \mathbf{r}_{\ell}) V(\mathbf{r}'), \quad (12)$$

where V^+ is the volume above the $\alpha\beta$ interface. Here we use the same notation introduced in [11] that a black dot above (below) a surface denotes an integral over the volume above (below) it. A factor of κ is introduced in these volume integrals so that all the diagrams have the same dimensionality. All other diagrams have equivalent interpretations.

Similarly, in the region below the $\alpha\beta$ interface, one can express the profile in a diagrammatic manner:

$$\begin{aligned} m(\mathbf{r}) &= m^{(0)}(\mathbf{r}) + \frac{\epsilon}{2\kappa^2} \left[\text{---} \text{---} - \text{---} \text{---} - \text{---} \text{---} + \text{---} \text{---} \right. \\ &\quad \left. + \text{---} \text{---} - \text{---} \text{---} - \text{---} \text{---} + \dots \right] \end{aligned} \quad (13)$$

where $m^{(0)}(\mathbf{r})$ is the solution for $\epsilon = 0$, given by [10]

$$\begin{aligned} m(\mathbf{r}) - m_0 &= \delta m_1 \text{---} \text{---} + m_0 \text{---} \text{---} + \delta m_1 \text{---} \text{---} + \dots \\ &\quad - (m_0 \text{---} \text{---} + \delta m_1 \text{---} \text{---} + m_0 \text{---} \text{---} + \dots). \end{aligned} \quad (14)$$

Here, $\delta m_1 = m_1 - m_0$, and the dots represent higher-order terms that ‘zig-zag’ between the interface and the substrate. The meaning of the diagrams is the same as that described above, with each diagram representing a multi-dimensional surface integral involving Green’s function K . For example

$$\text{---} \text{---} = \int ds_{\ell} \int ds_{\psi} K(\mathbf{r}_{\ell}, \mathbf{r}_{\psi}) K(\mathbf{r}_{\psi}, \mathbf{r}). \quad (15)$$

Again in the final set of diagrams of (13), the black dot located between the wavy lines signifies an integration over the volume of the adsorbed layer V^- (with a multiplicative factor of κ , for dimensional consistency). For example

$$\text{---} \text{---} = \int ds_{\ell} K(\mathbf{r}, \mathbf{r}_{\ell}) \int_{V^-} d\mathbf{r}' \kappa K(\mathbf{r}', \mathbf{r}_{\ell}) V(\mathbf{r}'). \quad (16)$$

Having found the constrained profiles, one can substitute these into (6) to determine the interfacial Hamiltonian. However, a more direct route is to use the Feynman–Hellman-like theorem [11]:

$$\frac{\partial H[\ell, \psi]}{\partial \epsilon} = -\frac{1}{\kappa} \int d\mathbf{r} \kappa m V(\mathbf{r}), \quad (17)$$

which can be integrated to get the same result. The interfacial Hamiltonian is

$$H[\ell, \psi] = \Sigma A_{\alpha\beta} + W[\ell, \psi] \quad (18)$$

where Σ is the surface tension of the (isotropic) $\alpha\beta$ interface and $A_{\alpha\beta} = \int ds_{\ell}$ is its area. The binding potential functional is given by

$$W[\ell, \psi] = W^{(0)}[\ell, \psi] + \frac{2m_0\epsilon}{\kappa} \text{---} \text{---} + \frac{\epsilon}{\kappa} W^{(1)} + \frac{\epsilon^2}{4\kappa^3} W^{(2)}. \quad (19)$$

This expression is exact for planar interfacial (and wall) configurations and is accurate to exponential order in the radii of curvature for spherical configurations. We have ordered the contributions into four sets of diagrams whose interpretation is as follows: the first contribution is the NL binding potential functional for $V(\mathbf{r}) = 0$, determined in [10]:

$$W^{(0)}[\ell, \psi] = 2\kappa m_0 \delta m_1 \text{---} \text{---} + \kappa m_0^2 \text{---} \text{---} + \dots, \quad (20)$$

where

$$\mathcal{Z} = \int \int ds_\psi ds_\ell K(\mathbf{r}_\psi, \mathbf{r}_\ell) \quad (21)$$

and

$$\mathcal{V} = \int \int \int ds_\ell ds_\psi ds'_\ell K(\mathbf{r}_\ell, \mathbf{r}_\psi) K(\mathbf{r}_\psi, \mathbf{r}'_\ell) \quad (22)$$

represent the leading-order contributions. All other diagrams in $W^{(0)}$ involve higher-order multiple surface integrals over K represented simply by adding additional thick lines that zig-zag between the surfaces. These contributions resum to yield a hard repulsion of the interface from the wall but can be otherwise ignored [10]. The second contribution, coming from a single diagram, may be regarded as that arising most directly from the external field:

$$\frac{2m_0\epsilon}{\kappa} \text{diagram} = 2m_0\epsilon \int_{V^+} d\mathbf{r} V(\mathbf{r}). \quad (23)$$

This is the term that would follow from taking the usual sharp-kink approximation to the interfacial profile [1] if we assumed the $\alpha\beta$ interface abruptly separates regions of bulk α - and β -like phases. Finally $W^{(1)}$ and $W^{(2)}$ represents first-order and second-order corrections to the direct sharp-kink approximation arising from the interaction of the external field and the exponentially decaying, or ‘soft’, tails of the profile:

$$\begin{aligned} W^{(1)} = & -m_0 \text{diagram} + \delta m_1 \text{diagram} \\ & - \left(\delta m_1 \text{diagram} + m_0 \text{diagram} + \delta m_1 \text{diagram} + \dots \right) \\ & + m_0 \text{diagram} + \delta m_1 \text{diagram} + m_0 \text{diagram} + \dots, \end{aligned} \quad (24)$$

$$\begin{aligned} W^{(2)} = & 2 \text{diagram} + \text{diagram} - \text{diagram} + \text{diagram} + \text{diagram} - 2 \text{diagram} \\ & + \text{diagram} + \text{diagram} - 2 \text{diagram} + \dots \end{aligned} \quad (25)$$

where the single surface diagrams (representing an interface infinitely far from the wall) are added so that $W^{(1)}$ and $W^{(2)}$ go to zero as $\ell \rightarrow \infty$. The new expression for the binding potential functional in the presence of an external field is certainly more complex than in the original NL model (1). However, the diagrammatic structure is quite clear and, for our specific applications, we have found that most of the new diagrams can be evaluated explicitly. In particular, a closed expression (not an expansion) can be calculated for the binding potential at mean-field level, both for planar and curved substrates (spheres and cylinders) allowing the identification of curvature corrections [19].

3. Three applications


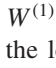
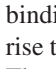
3.1. Constant external field

In the simplest application, the external potential represents, not a substrate–fluid interaction, but rather a constant (negative) bulk ordering field, i.e. $\epsilon V(\mathbf{r}) \equiv h$. Then, we find the expected expression

$$W[\ell, \psi] = W^{(0)}[\ell, \psi] - 2m_0 h V^- + \dots \quad (26)$$

where V^- is the volume of the wetting layer and a constant term has been subtracted. The correction to $W^{(0)}$, which arises from the analogue of the sharp-kink term, simply represents the thermodynamic penalty of having a wetting film of the metastable phase β . All the contributions from $W^{(1)}$ and $W^{(2)}$ are completely irrelevant, as they are exponentially small in the wetting layer thickness. The consequences of non-locality for complete wetting were explored before [12, 13].

3.2. Long-ranged forces

Now, suppose that the substrate is planar and gives rise to a long-ranged algebraically decaying potential $V(\mathbf{r}) = z^{-3}$, with z the normal distance to the wall. For long-ranged forces the upper critical dimension is always less than three so non-locality is not expected to bring any new qualitative effects. We can, however, check this explicitly. In this case, the dominant diagrams are the sharp-kink term , and the first-order terms  and , appearing in $W^{(1)}$, which are the ‘soft-kink’ corrections. These generate the leading-order algebraically decaying contributions to the binding potential (functional). The diagrams in $W^{(2)}$ also give rise to algebraically decaying terms, but these are higher order. The diagrams in $W^{(0)}$ are all exponentially decaying. In this way, we find the functional

$$W[\ell] = m_0\epsilon \int d\mathbf{x} \ell(x)^{-2} + \frac{4m_0\epsilon}{\kappa^2} \int ds \ell(x)^{-4} + \dots, \quad (27)$$

where $ds = \sqrt{1 + (\nabla\ell)^2} d\mathbf{x}$. Note that this expression involves both $d\mathbf{x}$ and ds integrals, which are testimony to the NL structure of the functional and are taken as equivalent in local approaches. Note that, if one removes the assumption of Ising symmetry for the bulk phases, then the same diagrams in $W^{(1)}$ also generate a correction of order ℓ^{-3} .

One may check this result against earlier predictions for a planar interfacial configuration of constant thickness ℓ_0 [15], in which, of course, $d\mathbf{x} = ds$. In this specific case, the binding potential functional can be written as

$$W[\ell] = A_{\alpha\beta} W(\ell_0) \quad (28)$$

which defines the usual *local* binding potential *function* $W(\ell_0)$. Dietrich and Napiórkowski [15] determined the form of this function for both long-ranged wall–fluid and fluid–fluid interactions. However, when the fluid–fluid interaction is short-ranged, and one assumes Ising symmetry, one can easily check that their equation (2.30), together with coefficients (2.31)–(2.37) are equivalent to $W(\ell_0) = m_0\epsilon\ell_0^{-2} + \frac{4m_0\epsilon}{\kappa^2}\ell_0^{-4} + \dots$ which is, of course, in agreement with the present theory.

3.3. The NL Aukrust–Hauge model

For our final example, we follow Aukrust and Hauge and choose a planar wall with an exponentially decaying potential of the form [16]

$$V(\mathbf{r}) = e^{-\lambda z}, \quad (29)$$

where z is, again, the normal distance to the wall. This potential is particularly interesting for wetting. Studies based on *local* interfacial Hamiltonians predict that the transition is first order for $\lambda < \kappa$, while, for $\lambda > \kappa$, it is second order (critical) with remarkable non-universal properties. Here, we seek to understand if non-locality influences these predictions, concentrating on the case of most theoretical interest, $\lambda > \kappa$. For the exponential potential, many of the diagrams can be evaluated exactly and we find

$$W[\ell] = a \text{---} \text{---} + b \text{---} \text{---} + c \text{---} \text{---} + d \text{---} \text{---} + \dots, \quad (30)$$





with coefficients given by

$$a = 2\kappa m_0 \delta m_1 + \frac{2\epsilon\kappa m_0}{\lambda^2 - \kappa^2} \quad (31)$$

$$b = \kappa m_0^2 \quad (32)$$

$$c = 2\epsilon m_0 \quad (33)$$

$$d = -\frac{2\epsilon\lambda m_0}{\lambda^2 - \kappa^2}. \quad (34)$$

The four contributions to this functional can be understood as follows: the second diagram is the same as the second diagram in $W^{(0)}$, and represents a repulsion from the wall, independent of the external field. The third diagram is simply the sharp-kink term, i.e. the direct influence of the external field. The remaining diagrams have contributions from different terms. For example, the first diagram arises from the first term of $W^{(0)}$, , and two diagrams of $W^{(1)}$,  and . The final term in (30) arises from the first diagram in $W^{(1)}$, .

3.3.1. Local approach. If the interface is flat, corresponding to a uniform wetting film of thickness ℓ , the binding potential function (28) is

$$W(\ell) = ae^{-\kappa\ell} + be^{-2\kappa\ell} + \left(\frac{c}{\lambda} + d\right)e^{-\lambda\ell} + \dots \quad (35)$$

The minimum of this binding potential determines the mean-field wetting film thickness $\bar{\ell}$. This function is also an essential ingredient in the standard local interfacial Hamiltonian, which we refer to as the capillary wave (CW) model:

$$H_{\text{CW}}[\ell] = \int d\mathbf{x} \left\{ \frac{\Sigma}{2} (\nabla\ell)^2 + W(\ell) \right\}, \quad (36)$$

valid for wavelengths $0 \leq q < \Lambda$, where $\Lambda \approx \kappa$ is the high momentum cutoff. If one considers small, Gaussian, fluctuations about the height $\bar{\ell}$, we may determine the mean-field expression for the height–height correlation function. The Fourier transform of this is defined as

$$G(q) \equiv \int d\mathbf{x}_{12} \delta\ell(\mathbf{x}_1) \delta\ell(\mathbf{x}_2) e^{i\mathbf{q}\cdot\mathbf{x}_{12}} \quad (37)$$

where $\delta\ell(\mathbf{x}) = \ell(\mathbf{x}) - \bar{\ell}$. For the CW model, the mean-field expression for $G(q)$ follows directly from equipartition:

$$G_{\text{CW}}(q) = \frac{k_B T}{W''(\bar{\ell}) + \Sigma q^2} \quad (38)$$


identifying a parallel correlation length $\xi_{\parallel} = \sqrt{\Sigma/W''(\bar{\ell})}$. Within the CW theory, this is also the true correlation length determining the large distance decay of the height–height correlation function. The simple Lorentzian form of the structure factor (38), characteristic of classic Ornstein–Zernike theory, indicates that within the CW description there is only one diverging length parallel to the wall.

Using the binding potential (35), we therefore conclude the following for the MF critical wetting behaviour. If $\lambda > 2\kappa$, the repulsive term of order $e^{-\lambda\ell}$ is unimportant and the critical wetting transition (which occurs as $a \rightarrow 0^-$) exhibits the same critical singularities as systems with short-ranged forces. For example, $\xi_{\parallel} \sim a^{-1}$, which identifies the well-known MF value of the critical exponent $\nu_{\parallel}^{\text{MF}} = 1$. If, instead, $\kappa < \lambda < 2\kappa$, the term of order $e^{-2\kappa\ell}$ is unimportant and the repulsion from the wall is determined by the external field. The critical wetting transition still occurs as $a \rightarrow 0^-$, but is now characterized by non-universal critical exponents, in particular, $\nu_{\parallel}^{\text{MF}} = \lambda/(2(\lambda - \kappa))$. Finally, if $\lambda < \kappa$, the external field term is dominant and any wetting transition is first order.

The influence of fluctuations on this MF behaviour was considered by Hauge and Olaussen [20] using renormalization group analysis of the CW model. The upper critical dimension for the transition remains $d = 3$, just as for systems with strictly short-ranged forces and, at this marginal dimension, interfacial fluctuations lead to non-universality controlled by the wetting parameter ($\omega = \kappa^2 k_B T / 4\pi \Sigma \alpha_{\beta}$). They find

$$\nu_{\parallel}(\omega) = \begin{cases} \frac{\nu_{\parallel}^{\text{MF}}}{1 - (\lambda/2\kappa)\omega} & \text{for } 0 < \omega < 2(\kappa/\lambda)^2 \\ (\sqrt{2} - \sqrt{\omega})^{-2} & \text{for } 2(\kappa/\lambda)^2 < \omega < 2 \end{cases} \quad (39)$$

and a strong fluctuation regime for $\omega > 2$, for which ξ_{\parallel} diverges exponentially. Only for the first regime $0 < \omega < 2(\kappa/\lambda)^2$ are the results different from the non-universality predicted for short-ranged forces by Brézin *et al* [4], whose results are recovered by setting $\lambda = 2\kappa$.

3.3.2. Non-local approach. In the absence of an external field, non-locality does not change the asymptotic critical behaviour of systems with short-ranged forces, but it modifies strongly the approach to the critical regime and, hence, the observability of non-universality. It also explains why the transition is not driven first order by fluctuation effects, as predicted by some local theories. Non-locality arises from the  diagram in the binding potential functional, which introduces another diverging parallel length scale characterizing a two-body interfacial interaction. Using a convolution to integrate over the point on the substrate one can write

$$\text{---} \text{---} = \int \int ds_1 ds_2 U(|x_2 - x_1|; \bar{\ell}) \quad (40)$$

with $2\bar{\ell} = \ell(x_1) + \ell(x_2)$ and

$$U(x; \ell) = \frac{\kappa^2}{2\pi} \int_{2\kappa\ell}^{\infty} d\tau \frac{e^{-\sqrt{\tau^2 + \kappa^2} x}}{\sqrt{\tau^2 + \kappa^2} x^2} \quad (41)$$

is a two-body interfacial interaction. For thick wetting films, this diagram reduces to

$$\mathcal{V} \approx \int \int ds_1 ds_2 e^{-\kappa \ell(x_1)} S(|x_2 - x_1|) e^{-\kappa \ell(x_2)} \quad (42)$$

where $S(|x_2 - x_1|)$ is another two-body interfacial interaction:

$$S(x) = \frac{1}{4\pi \xi_{\text{NL}}^2} e^{-x^2/4\xi_{\text{NL}}^2}, \quad (43)$$

which has the form of a simple Gaussian. The characteristic length of the Gaussian is identified as

$$\xi_{\text{NL}} = \sqrt{\frac{\bar{\ell}}{\kappa}}. \quad (44)$$

As shown in [9, 13, 14], this length scale serves to cut off the spectrum of interfacial fluctuations that interact with the wall (in the repulsive term), leading to a very slow onset of non-universality. This is consistent with Ising model simulation studies of critical wetting, which only revealed small deviations from MF-like expectations [6–8].

Upon inclusion of the external field (29), one might expect similar behaviour for the case of $\lambda > 2\kappa$, since the diagram \mathcal{V} (of order $\exp(-2\kappa\ell)$) [10] controls the interfacial repulsion from the wall and the external field term is higher order. However, it is not clear to what extent non-locality influences the non-universality in the regime $\kappa < \lambda < 2\kappa$. This is our concern here.

Non-locality arises in two ways: through the binding potential functional $W[\ell]$ and through the functional relation between the order parameter m and the collective coordinate ℓ . Let us consider each term in the binding potential functional (30). As noted above, the diagram \mathcal{V} is strongly non-local and is characterized by the same two-body interfacial interaction $S(x)$ and parallel length scale ξ_{NL} . The other three diagrams evaluate as follows:

$$\text{Diagram 1} = \int ds e^{-\kappa \ell} \quad (45)$$

$$\text{Diagram 2} = \frac{1}{\lambda} \int dx e^{-\lambda \ell} \quad (46)$$

$$\text{Diagram 3} = \int ds e^{-\lambda \ell}, \quad (47)$$

which are all local in character. From this, we conclude that the binding potential functional can be approximated as

$$W[\ell] = \int dx \left\{ a e^{-\kappa \ell(x)} + \left(\frac{c}{\lambda} + d \right) e^{-\lambda \ell(x)} \right\} + \int \int dx_1 dx_2 e^{-\kappa \ell(x_1)} S(|x_2 - x_1|) e^{-\kappa \ell(x_2)} \quad (48)$$

where irrelevant terms of order $\mathcal{O}(e^{-\kappa \ell} (\nabla \ell)^2)$ and $\mathcal{O}(e^{-\lambda \ell} (\nabla \ell)^2)$, arising from the gradient expansion of ds , have been dismissed.

Therefore, in the regime $\kappa < \lambda < 2\kappa$, one might be tempted to conclude that NL effects are unimportant (since the leading-order terms of the binding potential are, indeed, local)

and non-universal critical effects are more easily observed than in the regime $\lambda > 2\kappa$. However, this argument is wrong for two reasons. Firstly, it neglects fluctuation effects. For example, for $\omega > 2(\kappa/\lambda)^2$, the renormalized two-body interfacial interaction is of the same order as the renormalized local repulsion. Secondly, and more importantly, the approach to the asymptotic critical regime is strongly influenced by non-locality, even for $\omega < 2(\kappa/\lambda)^2$. One can see this readily in the MF correlation function structure and, by extension, in the Ginzburg criterion.

Following the analysis given in [12], it is straightforward to calculate the MF pair correlation function $G(\mathbf{r}_1, \mathbf{r}_2) = \langle m(\mathbf{r}_1)m(\mathbf{r}_2) \rangle - \langle m(\mathbf{r}_1) \rangle \langle m(\mathbf{r}_2) \rangle$ for the microscopic Hamiltonian (2). The result for the singular contribution of the parallel Fourier transform $\mathcal{G}(z_1, z_2; q)$, when both particles are near the wall, is given by

$$\mathcal{G}(0, 0; q) \approx \frac{e^{-2\kappa \ell} e^{-q^2 \bar{\ell}/\kappa}}{E + \Sigma q^2}, \quad (49)$$

where

$$E = a\kappa^2 e^{-\kappa \ell} + (c\lambda + d\lambda^2) e^{-\lambda \ell} + 4b\kappa^2 e^{-2\kappa \ell} S(q) \quad (50)$$

and $S(q) = e^{-\xi_{\text{NL}}^2 q^2}$, is the Fourier transform of the two-body interaction.

Thus, even in the regime $\kappa < \lambda < 2\kappa$, where the final term in E related to the two-body term is unimportant, the numerator in $\mathcal{G}(0, 0; q)$ is still strongly damped for $q > 1/\xi_{\text{NL}}$. This is because the functional relation between fluctuations in m and ℓ is still non-local [12]. This damping is not captured by local approaches, but is modelled correctly by the NL Hamiltonian. This has an immediate implication for the calculation of the Ginzburg criterion concerning the self-consistency of MF theory. Following the argument given in [12], we conclude that MF theory is valid (in 3D) provided the condition

$$\frac{\kappa^2}{2\pi} \int_0^\Lambda dq \frac{q e^{-q^2 \xi_{\text{NL}}^2}}{E + \Sigma q^2} \ll 1 \quad (51)$$

is fulfilled. The interpretation of this is almost exactly the same as for systems with short-ranged forces. The damping in the numerator effectively lowers the momentum cutoff from Λ to $1/\xi_{\text{NL}}$. One way of understanding this is through the concept of an effective wetting parameter ω_{eff} , whose value depends on the thickness of the wetting layer. Performing the integral above, one may re-express the Ginzburg criterion for the NL model as

$$\ln(1 + \Lambda^2 \xi_{\parallel}^2) \ll \frac{1}{\omega_{\text{eff}}} \quad (52)$$

where the effective value of the wetting parameter is

$$\omega_{\text{eff}} = \omega \frac{\ln(1 + \Lambda_{\text{NL}}^2 \xi_{\parallel}^2)}{\ln(1 + \Lambda^2 \xi_{\parallel}^2)}. \quad (53)$$

Even for relatively thick wetting layers, several bulk correlation lengths thick, ω_{eff} is much smaller than its asymptotic value ω . This can be seen explicitly [13]. For

example, in regime II the RG result $\kappa\ell \approx \sqrt{2\omega} \ln(\Lambda^2 \xi_{\parallel}^2)$ and $\Lambda_{\text{NL}} \approx \sqrt{\kappa/\ell}$ leads to

$$\omega_{\text{eff}} \approx \omega \frac{\ln(1 + (\kappa/\ell\Lambda^2)e^{\kappa\ell/\sqrt{2\omega}})}{\ln(1 + e^{\kappa\ell/\sqrt{2\omega}})}. \quad (54)$$

3.3.3. Simulations. To test the above reasoning, we have performed Monte Carlo simulations of discretized versions of two interfacial models. The first is a standard local CW model:

$$H_{\text{CW}} = \int d\mathbf{x} \left\{ \frac{\Sigma}{2} (\nabla\ell)^2 + \bar{h}\ell + \left(\frac{c}{\lambda} + d \right) e^{-\lambda\ell} + b e^{-2\kappa\ell} \right\}, \quad (55)$$

where $\bar{h} = 2m_0|h|$. The second is the analogous NL Hamiltonian:

$$H_{\text{NL}} = \int d\mathbf{x} \left\{ \frac{\Sigma}{2} (\nabla\ell)^2 + \bar{h}\ell + \left(\frac{c}{\lambda} + d \right) e^{-\lambda\ell} \right\} + b \nabla^2, \quad (56)$$

where the final diagram is evaluated as the two-body interaction U . These models differ only in the sub-leading-order term ($O(e^{-2\kappa\ell})$); this term is local in the first model and non-local in the latter. Since the leading-order terms are the same we expect the asymptotic behaviour to be equal for both models. However, as reasoned in section 3.3.2, the approach to the critical regime will be strongly influenced by non-local effects for wetting layers of finite thickness. Provided the wetting parameter $\omega < 2$, both models describe the approach to the critical wetting transition from off-coexistence, exactly at the wetting temperature, equivalent to setting $a = 0$. The approach to critical wetting is done from off-coexistence to allow an easier comparison with earlier work [9, 10, 13, 21]. In this previous work the main concern was the comparison with Ising model simulations [6, 7] for which the approach from off-coexistence allows the measurement of ν_{\parallel} through the use of the relation

$$\langle \Delta m_1 \rangle \sim \langle e^{-\kappa\ell} \rangle \sim |\bar{h}|^{1-1/\nu_{\parallel}}. \quad (57)$$

Our reasoning from section 3.3.2 remains valid for this approach to critical wetting as the main effect of non-locality is in the numerator of (49), and this remains the same off-coexistence. We already explored previously the effects of non-locality for a finite bulk field and at complete wetting [13].

We follow essentially the same methodology (described briefly below) used in previous work: for a more detailed discussion we refer to [13, 21]. We discretize the models in a lattice of size $L \times L$ with periodic boundary conditions and lattice spacing $\delta = 3.1623/\kappa$. In each Monte Carlo step, we choose a lattice site i at random and increment the interfacial height $\ell(x_i)$ by a random number which follows a uniform probability distribution on the interval $[-\Delta\ell, \Delta\ell]$. Finally, we use the usual Metropolis algorithm [22] to accept or reject the new configuration. $\Delta\ell$ is chosen so that approximately 40%–50% of the attempted configurations are accepted. The averages were evaluated over about 10^5 (10^6) Monte Carlo steps per site, after an equilibration period of 10^4 (10^5) Monte Carlo steps per site for $L/\delta = 101$ (201). Applying the scaling relation (57) to our data, we are able to extract an effective

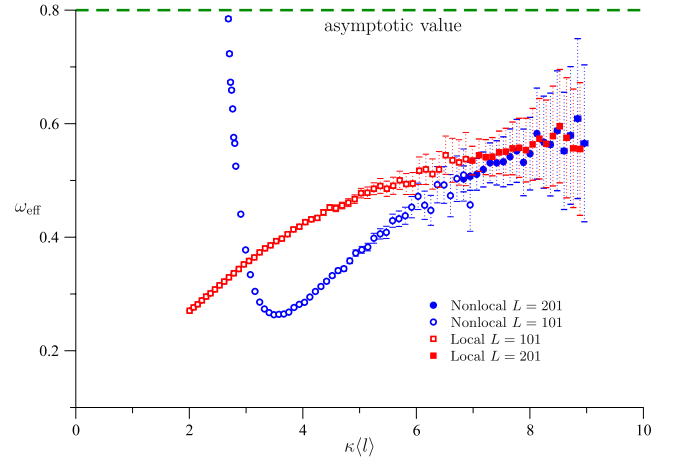


Figure 2. Monte Carlo simulation results for the effective value of the wetting parameter ω_{eff} , as a function of the film thickness $\kappa(\ell)$, for the local (equation (55), red squares) and non-local (equation (56), blue circles) versions of the Aukrust–Hauge model in regime II. Simulations on an $L \times L$ grid, where L is measured in units of $3.1623/\kappa$, $\lambda = 1.75\kappa$ and $b = 2.5\kappa^2 k_B T$.

value of the correlation length exponent ν_{\parallel} and, from (39), determine an effective value of the wetting parameter, which we can plot against the equilibrium film thickness.

For our model parameters, we set $\omega = 0.8$ and $b = 2.5\kappa^2 k_B T$ which are reasonable Ising-like parameters, and $\frac{c}{\lambda} + d = b$, so that the amplitudes of the local and non-local terms are of the same magnitude to make any effect of the non-local term more transparent. For the external field, we have considered the values $\lambda = 1.4\kappa$ and 1.75κ , which are in the first and second fluctuation regimes, respectively. Thus, according to the renormalization group predictions, we anticipate that $\nu_{\parallel} = 3.98$ and 3.70 , respectively.

In both cases, we find that non-locality has a significant influence on the predicted non-universality. For $\lambda = 1.75\kappa$, the results are similar to those obtained for systems with short-ranged forces ($V = 0$). This is illustrated in figure 2, where we plot the effective value of the wetting parameter versus the averaged film thickness. The characteristic shape of ω_{eff} in this regime is very similar to that obtained in earlier simulations: in particular, there is a minimum value $\omega_{\text{eff}} \approx 0.3$ for wetting films about four bulk correlation lengths thick. In our simulations, the effective value of ω is substantially smaller than 0.8, even for our thickest wetting layers. For $\lambda = 1.4\kappa$, on the other hand, the description based on an effective value of ω breaks down completely for thin wetting films and ω_{eff} can even become negative. This is due to a very pronounced ‘bump’ in the values of $\langle e^{-\kappa\ell} \rangle$ as a function of the bulk field, showing a strong signature of (sub-leading-order) non-local effects for thin wetting films, see figure 3.

4. Conclusions

In this paper, we have extended our earlier derivations of an NL interfacial model from an underlying microscopic Hamiltonian. Our analysis is still limited to systems with short-ranged fluid–fluid forces, but now it incorporates an

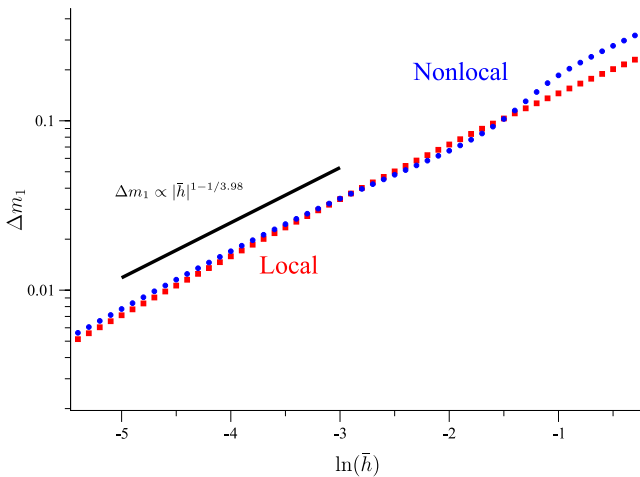


Figure 3. Monte Carlo simulation results for the surface magnetization-like operator $\Delta m_1 = \langle e^{-\kappa l} \rangle$ with the bulk field \bar{h} for the local (equation (55), red squares) and non-local (equation (56), blue circles) versions of the Aukrust–Hauge model in regime I. The black line is the predicted asymptotic result $\nu_{\parallel} = 3.98$, where only the slope matters. Simulations on an 101×101 grid, measured in units of $3.1623/\kappa$, $\lambda = 1.4\kappa$ and $b = 2.5\kappa^2 k_B T$.

arbitrary external potential $V(\mathbf{r})$. The first thing to note is that the diagrammatic Green’s function method introduced in [10], does generalize to this case. The binding potential functional $W[\ell, \psi]$ describing the interaction of the interface and the wall still has a diagrammatic representation, but now includes extra terms due to the external field. Even though there are an infinite number of new diagrams, these can be ordered in a relatively simple manner. There is, for example, a single ‘sharp-kink’ diagram, which accounts for the most direct influence of the external field and which, in many circumstances, is the dominant interaction. Thus, we feel that our derivation lends strong support to previous studies based on phenomenological interfacial Hamiltonians. The remaining two classes of diagrams, which describe first-order and second-order interactions between the external field and the intrinsic structure, can be ordered into sets of ‘zig-zag’ diagrams containing higher numbers of kernels which stretch between the interface and wall. The structure of these is similar to that found for systems with purely short-ranged forces, except there is an extra kernel for $W^{(1)}$ and two kernels for $W^{(2)}$ associated with the external field.

In this paper, we have also restricted our attention to the double-parabola approximation for the bulk thermodynamic potential $\Delta\phi(m)$. Using the methods described in [11], one could in principle extend the derivation to more general types of potential, although the enumeration and ordering of the additional diagrams, which would include third-, fourth- and higher-order coupling to the external field, would be quite daunting. We do not anticipate that this would reveal any new physics.

Besides the inclusion of a constant external field, we have considered two applications of the present formalism. The first was the case of a long-ranged algebraically decaying potential $V = 1/z^3$, where we were able to make a connection with earlier work by Dietrich and Napiórkowski [15], supporting

many of their conclusions. The second application was the case of an exponentially decaying substrate potential similar to a model introduced by Aukrust and Hauge [16]. The nature of the critical wetting transition in this model is very subtle, not only because the upper critical dimension is $d = 3$, but also because non-universality can arise at the MF level in itself. We have shown that NL effects are still highly important for this model, even in regimes where it appears that the leading terms in the binding potential functional are local. Our analysis is fully supported by Monte Carlo simulations, where sub-leading-order non-local terms are seen to have a strong influence on the approach to the wetting transition. In regime I these effects are so strong that an attempt to extract an effective wetting parameter ω_{eff} leads to negative values for thin wetting layers. The results of this work strengthen the conclusion of our earlier studies of critical wetting in systems of SR forces; namely, that non-universality might be present asymptotically but NL effects associated with the additional length scale ξ_{NL} dampen interfacial fluctuations.

Acknowledgments

We thank Professor Dietrich and Dr Tasinkevych for a critical reading of the manuscript and help with the simulations. NRB acknowledges partial support from the Portuguese Foundation for Science and Technology (SFRH/BD/16424/2004). CR acknowledges support from grants MOSAICO (Ministerio de Educación y Ciencia) and grant CCG08-UC3M/ESP-4499 (Comunidad de Madrid/UC3M). JMR-E acknowledges support from Junta de Andalucía through grant P06-FQM-01869.

References

- [1] Dietrich S 1988 *Phase Transitions and Critical Phenomena* vol 12, ed C Domb and J Lebowitz (New York: Academic)
- [2] Forgacs G, Lipowsky R and Nieuwenhuizen T M 1991 *Phase Transitions and Critical Phenomena* vol 14, ed C Domb and J Lebowitz (New York: Academic)
- [3] Bonn D, Eggers J, Indekeu J, Meunier J and Rolley E 2009 *Rev. Mod. Phys.* **81** 739
- [4] Brézin E, Halperin B I and Leibler S 1983 *Phys. Rev. Lett.* **50** 1387
- [5] Fisher D S and Huse D A 1985 *Phys. Rev. B* **32** 247
- [6] Binder K, Landau D P and Kroll D M 1986 *Phys. Rev. Lett.* **56** 2272
- [7] Binder K, Landau D P and Wansleben S 1989 *Phys. Rev. B* **40** 6971
- [8] Parry A O, Evans R and Binder K 1991 *Phys. Rev. B* **43** 11535
- [9] Parry A O, Romero-Enrique J M and Lazarides A 2004 *Phys. Rev. Lett.* **93** 086104
- [10] Parry A O, Rascón C, Bernardino N R and Romero-Enrique J M 2006 *J. Phys.: Condens. Matter* **18** 6433
- [11] Parry A O, Rascón C, Bernardino N R and Romero-Enrique J M 2007 *J. Phys.: Condens. Matter* **19** 416105
- [12] Parry A O, Rascón C, Bernardino N R and Romero-Enrique J M 2008 *Phys. Rev. Lett.* **100** 136105
- [13] Parry A O, Romero-Enrique J M, Bernardino N R and Rascón C 2008 *J. Phys.: Condens. Matter* **20** 505102

-
- [14] Parry A O, Rascón C, Bernardino N R and Romero-Enrique J M 2008 *J. Phys.: Condens. Matter* **20** 494234
- [15] Dietrich S and Napiórkowski M 1991 *Phys. Rev. A* **43** 1861
- [16] Aukrust T and Hauge E H 1985 *Phys. Rev. Lett.* **54** 1814
- [17] Fisher M E and Jin A J 1991 *Phys. Rev. B* **44** 1430
- [18] Jin A J and Fisher M E 1993 *Phys. Rev. B* **47** 7365
- [19] Bernardino N R 2008 *PhD Thesis* Imperial College London
- [20] Hauge E H and Olaussen K 1985 *Phys. Rev. B* **32** 4766
- [21] Gomper G and Kroll D M 1988 *Phys. Rev. B* **37** 3821
- [22] Landau D P and Binder K 2005 *Monte Carlo Methods in Statistical Physics* 2nd edn (Cambridge: Cambridge University Press)